

# Mass and size effects on the transport properties of molten salts

Makoto Harada,<sup>a)</sup> Akihiro Yamanaka, Masataka Tanigaki, and Yutaka Tada<sup>b)</sup>

*Institute of Atomic Energy, Kyoto University, Uji, Kyoto, 611 Japan*  
(Received 19 August 1981; accepted 8 October 1981)

The mass and size dependencies of the ionic transport processes were studied by molecular dynamics calculations on the model fluid interacting through repulsive soft-core and the Coulomb potentials. The mass difference between anion and cation significantly affects the ionic transport processes. On the contrary, the change in the time evolution of the processes due to size difference between unlike ions is comparatively small. A perturbation treatment for the mass effect was developed to describe the velocity autocorrelation function, the electrical current autocorrelation function, and corresponding transport properties.

## I. INTRODUCTION

Ionic molten salts are regarded as binary mixtures composed of anions and cations, in which the interionic potential would be expressed by the rigid ion potential model proposed by Tosi-Fumi.<sup>1</sup> The dispersion force may play a minor role in the transport properties. In pure fluids, the mass and the size of the molecule are accounted as the scaling factors of time, momentum, and other variables.<sup>2</sup> In mixtures, the mass and size differences between unlike molecules play a significant role in the transport properties.<sup>3</sup> Even for the simple corresponding states correlation of the transport properties,<sup>4</sup> there is no logical method to take into account the effects of these two parameters.

Ciccotti<sup>5</sup> has reported the results of the molecular dynamics calculation for several alkali halides. In their calculation, the masses of the ions were changed together with the sizes of the ions in order to simulate the existing alkali halides. The effects of the mass and size differences were not separately evaluated. Lantelme<sup>6</sup> calculated the mass effect on self-diffusion process of the molten salt which interacted through the ion pair potential for sodium chloride.

This report aims at the elucidation of the mass and size effects on self-diffusion and electrical conduction processes, i. e., the mass effect is elucidated for the systems interacting through the Coulomb potential and the same core repulsion potential for the anion and the cation: The size effect is evaluated for the systems, the ions of which have a unique mass.

Next, we will be concerned with the perturbation approach to explain the mass effect on the transport properties. Schofield<sup>7</sup> has developed a perturbation theory for the binary mixtures in which the perturbation parameter was selected so that the Hamiltonian was invariant for the reference and the perturbed systems. In this report we apply the perturbation by Parrinello<sup>8</sup> to molten salts. The reference system is the one having a unique mass for the cation and the anion, twice the reduced mass of the unlike ion pair. The velocity autocorrelation function and its memory function are discussed

along with the electrical current autocorrelation function, with the help of the perturbation with respect to the mass difference. Finally, the effect of the mass difference on the self-diffusion coefficient and the electrical conductivity is discussed.

## II. MOLECULAR DYNAMICS CALCULATION

Molecular dynamics experiments for the univalent molten salts were performed using Verlet's algorithm.<sup>9</sup> All calculations were made for the system of 32 anions and 32 cations with periodical boundary conditions. The pair potential used is

$$\phi_{ij}(\gamma) = \lambda_{ij} e^{-\gamma/\sigma} + z_i z_j e^2/\gamma, \quad (1)$$

where  $z_i$  and  $e$  are the valence of the  $i$ th ion and the elementary charge, respectively. The first term in Eq. (1) represents the core repulsive potential. The parameters  $\lambda_{ij}$  and  $\sigma$  used to elucidate the mass difference effect were the values  $2.863 \times 10^{-9}$  erg and  $3.37 \times 10^{-9}$  cm. These values correspond to those for the core potential between the unlike ions of potassium chloride.<sup>1</sup> The experiment on the size effect was performed with unequal values of  $\lambda_{ij}$  and with a unique mass for the anion and the cation. The experimental conditions are listed in Table I. The force and the energy arising from the Coulomb potential were evaluated by the Ewald sum.<sup>10,11</sup>

The system treated in this report is regarded as a binary mixture comprised of the anion and the cation, and the total momentum of the system must be conserved:

$$\sum_j \mathbf{p}_j = 0. \quad (2)$$

When the initial momenta of the ions were selected so that Eq. (2) held, Eq. (2) was automatically satisfied in the successive time steps. The time step  $\Delta t$  was selected as  $5 \times 10^{-15}$  s for the system which consists of the anion and the cation of equal mass ( $m_A = m_C = m^* = 6.17 \times 10^{-23}$  g). For the systems having unequal ionic masses, the time step was  $5 \times 10^{-15} (2m_r/m^*)^{-1/2}$ ,  $m_r$  being the reduced mass for the unlike ion pair. The 8000 time steps were generated and the final 7000 steps were used for the averages.

The normalized velocity autocorrelation function (VACF) and the corresponding mean square displace-

<sup>a)</sup>To whom all correspondences should be addressed.

<sup>b)</sup>Now at Tottori University, Tottori, Japan.

ment (MSD) were calculated:

$$Z_\nu^v = \langle \mathbf{p}_i(\tau) \mathbf{p}_i(t + \tau) \rangle / \langle \mathbf{p}_i(\tau) \mathbf{p}_i(\tau) \rangle, \quad (3a)$$

$$\Delta D_\nu^v = \langle (\mathbf{r}_i(t + \tau) - \mathbf{r}_i(\tau))^2 \rangle, \quad i \in \text{ion species } \nu. \quad (3b)$$

The electrical current autocorrelation function (ECACF) and the corresponding mean square displacement (EMSD) were also calculated:

$$Z^e = \langle \mathbf{j}(t + \tau) \mathbf{j}(\tau) \rangle / \langle \mathbf{j}(\tau) \mathbf{j}(\tau) \rangle, \quad (4a)$$

$$\mathbf{j}(t) = \sum_i e z_i \mathbf{p}_i(t) / m_i,$$

$$\Delta D^e = \left\langle \left\{ \sum_i z_i [\mathbf{r}_i(t + \tau) - \mathbf{r}_i(\tau)] \right\}^2 \right\rangle. \quad (4b)$$

Here,  $m_i$  is the mass of the  $i$ th ion.

### III. EXPERIMENTAL RESULTS

#### A. Mass effect on self-diffusion process

The density  $\rho$  and the temperature  $T$  in the experiments are shown in Table I. In experiment M0 shown in Table I, all ions have the same mass and we call this the reference system. The internal energy and the compressibility factor of this system were

$$-U^*/NkT = 38.75, \quad p^*V/NkT = 1.71,$$

where the asterisk represents the value of the reference system. The conditions of calculation nearly correspond to the melting point for potassium chloride.

Figure 1(a) shows the VACF  $Z_\nu^v$  for the reference system. The shape of the VACF is similar to that of an inert gas molecule near its triple point.<sup>12</sup> From this VACF, the corresponding memory function  $K_\nu(t)$  can be evaluated from the generalized Langevin equation with the help of numerical Fourier transform<sup>13,14</sup>

$$dZ_\nu^v/dt + \int_0^t K_\nu(\tau) Z_\nu^v(t - \tau) d\tau = 0, \quad (5a)$$

$$K_\nu(t) = \langle \mathbf{f}_i(t) \mathbf{f}_i(0) \rangle / \langle \mathbf{p}_i(0)^2 \rangle, \quad i \in \nu, \quad (5b)$$

$$m_\nu K_\nu(0) = \frac{1}{2} \rho \left( \sum_\eta \int \nabla^2 \phi_{\nu\eta} g_{\nu\eta} d\mathbf{r} \right) \equiv F_\nu, \quad (5c)$$

where  $\mathbf{f}_i(t)$  is the random force acting on the  $i$ th ion, and  $g_{\nu\eta}$  is the radial distribution function for  $\nu - \eta$  ion pair. The  $F_\nu$  value for the reference system was  $2.81 \times 10^4$  g/s<sup>2</sup>. The normalized memory kernel  $K_\nu^*(t)/K_\nu^*(0)$  for the reference system is shown in Fig. 1(b) and this is also similar to that of an argon-like molecule near its

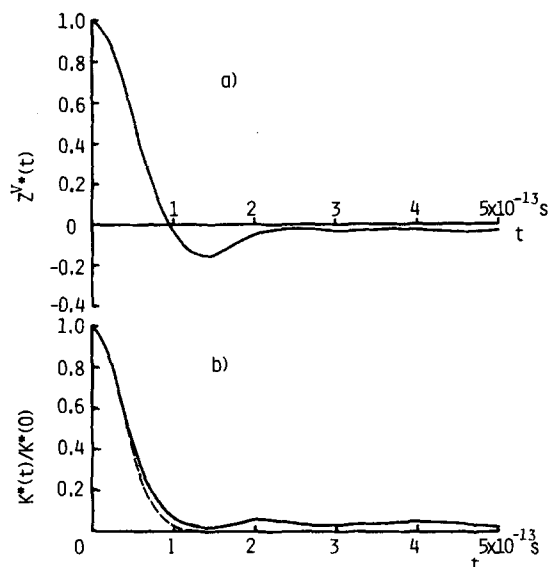


FIG. 1. Velocity autocorrelation function and its memory function for the reference system. (a) VACF, (b) normalized memory kernel. The solid curves are experimental results and the broken curve is the Gaussian function.

triple point.<sup>12</sup> The short time behavior of the memory kernel can be fitted to a Gaussian:

$$K_\nu^*(t) = K_\nu^*(0) \exp(-Bt^2), \quad B = 3.74 \times 10^{26} \text{ s}^{-2}. \quad (6)$$

As time proceeds, the memory kernel starts to deviate from the Gaussian and remains almost constant over a time period  $5 \times 10^{-13}$  s, after which it gradually decays to zero. In the molten salt system, the ions associate with each other due to the strong Coulomb force and this yields large holes in the system.<sup>15</sup> The long time tail would be related to the strong cooperative motions of the ions and the decay time of the tail would be connected with the time of the redistribution of the large holes.

The diffusion coefficient can be obtained from the VACF and also from the MSD:

$$D_\nu = \frac{kT}{m_\nu} \int_0^\infty Z_\nu^v(t) dt = \lim_{t \rightarrow \infty} \frac{1}{6t} \Delta D_\nu^v. \quad (7)$$

The results of the calculation at the conditions in Table I are shown in the table.

Figure 2 shows the effect of the mass difference on the VACF's. The abscissa is the modified time scaled as

TABLE I. Experimental conditions and data.

Run number	$T$ (K)	$\rho \times 10^{-22}$ (cm <sup>-3</sup> )	$\lambda_{AC} \times 10^9$ (erg)	$\lambda_{AA} \times 10^9$ (erg)	$\lambda_{CC} \times 10^9$ (erg)	$m_A/m_C$	$2m_\nu/m^*$	$\mu$	$D_C \times 10^5$ (cm <sup>2</sup> /s)	$D_A \times 10^5$ (cm <sup>2</sup> /s)	$\kappa \times 10^{-12}$ (s <sup>-1</sup> )
M0	967	2.077	2.863	2.863	2.863	1	1	0	6.25 <sup>a</sup> 6.16 <sup>b</sup>	6.25 <sup>a</sup> 6.16 <sup>b</sup>	2.21 <sup>b</sup>
M1	968	2.077	2.863	2.863	2.863	2	1	1/3	6.41 <sup>a</sup> 6.44 <sup>b</sup>	6.05 <sup>a</sup> 5.66 <sup>b</sup>	2.44 <sup>b</sup>
M2	966	2.077	2.863	2.863	2.863	5	1	4/6	6.26 <sup>a</sup> 6.17 <sup>b</sup>	5.28 <sup>a</sup> 5.41 <sup>b</sup>	2.33 <sup>b</sup>
M3	962	2.077	2.863	2.863	2.863	4	2/5	0.6	9.42 <sup>a</sup> 9.24 <sup>b</sup>	8.33 <sup>a</sup> 8.04 <sup>b</sup>	3.05 <sup>b</sup>
M4	955	2.077	2.863	2.863	2.863	10	20/11	9/11	4.17 <sup>a</sup> 4.17 <sup>b</sup>	2.86 <sup>a</sup> 2.95 <sup>b</sup>	1.27 <sup>b</sup>
M5	951	2.077	2.863	12.24	0.6702	1	1	0	6.01 <sup>a</sup> 6.14 <sup>b</sup>	5.13 <sup>a</sup> 4.99 <sup>b</sup>	2.19 <sup>b</sup>

<sup>a</sup>Values evaluated from VACF.

<sup>b</sup>Values evaluated from mean square displacement.

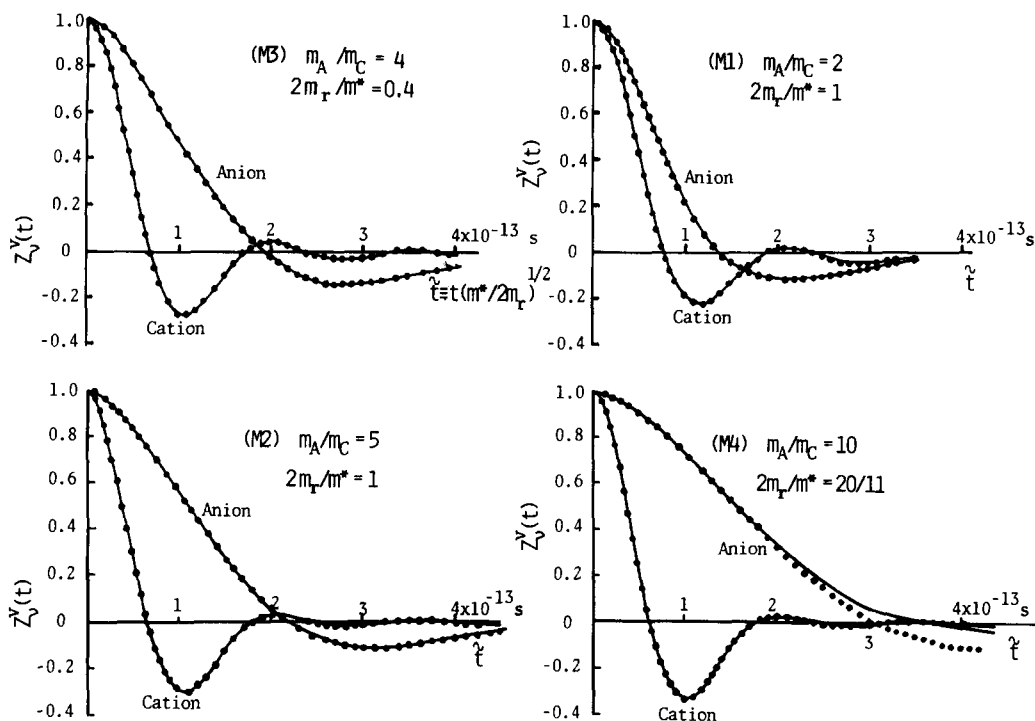


FIG. 2. Effect of mass difference between unlike ions on the velocity autocorrelation function. Keys: MD calculations; solid curve: calculated values by perturbation method.

$t(2m_r/m^*)^{-1/2} \equiv \tilde{t}$ . When one ion is significantly lighter than its partner ion, the VACF is oscillatory. The short time behavior of the VACF is reduced to a unique function irrespective of the mass difference if the time is scaled as  $t/m_v^{1/2}$  as Lantelme pointed out.<sup>6</sup> The normalized memory kernels are compared with that of the reference system in Fig. 3, where the abscissa is also  $\tilde{t}$ . The normalized memory kernels of the systems with unequal ion masses result in a unique Gaussian in shorter time irrespective of the reduced mass and the mass ratio  $m_A/m_C$  when time is scaled as  $\tilde{t}$ .

The large uncertainty resulting from the inversion of the Fourier transform of the VACF exists in the long time tail of the memory kernel. Taking this into account, the long time behavior of the memory kernel displays similar pattern to that of the reference system, when time is scaled as shown in the figure. Major effect of the mass difference on the memory kernel appears in the time interval  $6 \times 10^{-14} < \tilde{t} < 30 \times 10^{-14}$  s. This time range corresponds to the process that an ion interacts strongly with its neighboring shell.

### B. Effect of mass difference on electrical conductance

Figure 4 shows the effect of the mass difference on the normalized ECACF. The abscissa is scaled as  $\tilde{t}$ . The broken curve is the ECACF for the reference system. The electrical conduction process is not a singlet process but reflects a collective property and the short time expansion of the ECACF yields the relationship that the ECACF is a function of the scaled time  $\tilde{t}$ . This relation is satisfied in the experimental results. Even

in the longer time, the ECACF is insensitive to the mass difference.

The electrical conductivity  $\kappa$  can be evaluated from the integral of the ECACF or the EMSD:

$$\begin{aligned} \kappa &= \frac{1}{3kTV} \int_0^\infty \langle j(t)j(0) \rangle dt \quad (V: \text{volume of system}) \\ &= \lim_{t \rightarrow \infty} \frac{e^2}{6kTVt} \Delta D^p. \end{aligned} \quad (8)$$

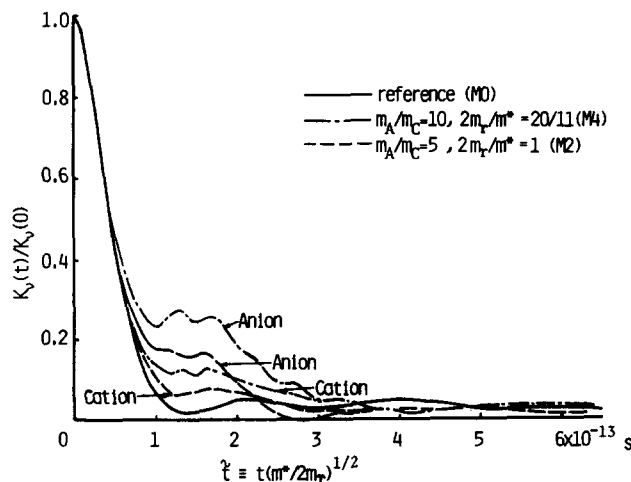


FIG. 3. Effect of mass difference between unlike ions on the memory kernel. The normalized memory kernels in the initial period result in a unique Gaussian irrespective of the mass difference when time is scaled as  $t(m^*/2m_r)^{1/2}$ .

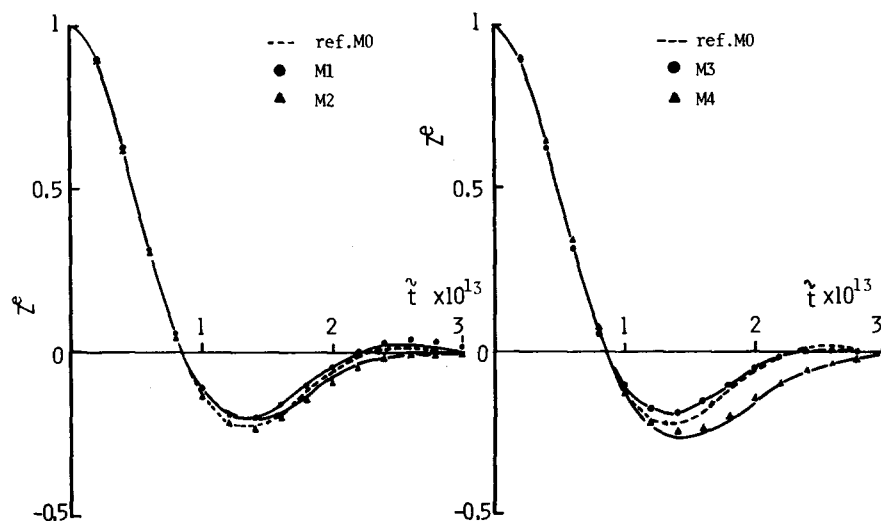


FIG. 4. Effect of mass difference on the electrical current autocorrelation function. The solid curves are calculated by the perturbation method.

The values of  $\kappa$  evaluated from the EMSD is more precise than that from the integral of the ECACF, because the ECACF in the long time range involves significant error. The electrical conductivities obtained are shown in Table I.

### C. Size effect on self-diffusion and electrical conduction

In this work the soft core repulsive potential was used and the strict diameters of the ions can not be evaluated. Since the parameter  $\lambda_{ij}$  is the index of the ion size, the parameters between the like ion pairs  $\lambda_{CC}$  and  $\lambda_{AA}$  were changed from that for the reference system, keeping  $\lambda_{AC}$  unchanged (condition M5). The normalized VACF and its memory kernel are compared with those of the reference system in Fig. 5. The core size effect on the self-diffusion process is very weak, reflecting the importance of the interaction between the unlike ions. The effect of ion size on the ECACF is also weak, as shown in Fig. 6.

## IV. ANALYSES OF THE MASS EFFECT BY PERTURBATION METHOD

As pointed out in the preceding section, the choice of a time scale  $\bar{t}$  is appropriate to describe the feature of

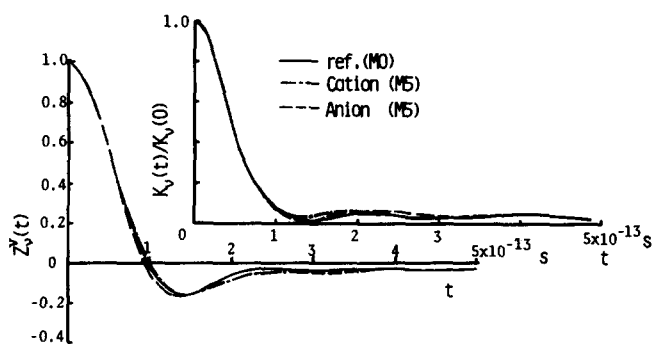


FIG. 5. Effect of ion size difference on the velocity autocorrelation function and its memory kernel.

the normalized memory kernel of the VACF. Up to  $\bar{t} = 6 \times 10^{-14}$  s, an exact superposition of the memory kernels is obtained for the systems with different masses of the unlike ions. At longer time periods, the memory kernels deviate from that of the reference system. This deviation becomes larger as the mass ratio of the ions  $m_A/m_C$  increases. These trends suggest the validity of the perturbation approach, in which the ions of the unperturbed system have a unique mass  $m_0 = 2m_r$  and the Hamiltonian and the evolution operator of the perturbed system are expressed by the sum of the unperturbed and the perturbed terms.

We consider a mixture of equal numbers of anion and cation, the total number of ions being  $N$ . The masses of the anion and the cation are  $m_A$  and  $m_C$ , respectively, and we choose the mass of the ions of the unperturbed system as  $m_0 = 2m_r$ . The Hamiltonian is given by

$$H = \sum_i \mathbf{p}_i^2 / 2m_i + \Phi^{(N)}, \quad \Phi^{(N)} = \sum_{i,j} \phi_{ij}, \quad (9)$$

where the pair potential is described by

$$\phi_{ij} = \lambda \exp(-r_{ij}/\sigma) + z_i z_j e^2 / r_{ij} = \Lambda \exp[(1 - \hat{r}_{ij})d/\sigma] + z_i z_j e^2 / (\hat{r}_{ij}d). \quad (10)$$

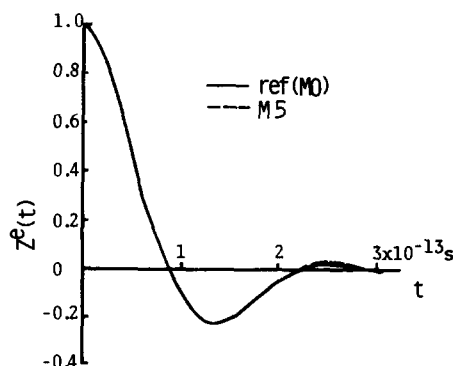


FIG. 6. Effect of size difference on the electrical current autocorrelation function.

The momentum and the position are scaled as

$$\hat{\mathbf{p}}_i = \mathbf{p}_i / (\Lambda m_0)^{1/2}, \quad \hat{\mathbf{r}}_i = \mathbf{r}_i / d, \quad \hat{r}_{ij} = r_{ij} / d. \quad (11)$$

The  $d$  value is an appropriate diameter of the ion.

The Hamiltonian can be rewritten in reduced form:

$$\hat{H} \equiv H / \Lambda = \hat{H}_0 + \Delta \hat{H}_m, \quad \hat{H}_0 = H_0 / \Lambda = \sum_i \hat{\mathbf{p}}_i^2 / 2 + \hat{\Phi}^{(N)},$$

$$\hat{\Phi}^{(N)} = \sum_{i>j} \left( \exp[(1 - \hat{r}_{ij})d/\sigma] + \frac{z_i z_j e^2}{\hat{r}_{ij} d \Lambda} \right),$$

$$\Delta \hat{H}_m = - \sum_i \mu_i \hat{\mathbf{p}}_i^2 / 2. \quad (12)$$

The perturbation parameter is expressed as

$$\mu_i = 1 - \frac{m_0}{m_i}. \quad (13)$$

The evolution operator  $L$  is

$$i\hat{L} = i \sum_i \left( \frac{\mathbf{p}_i}{m_i} \frac{\partial}{\partial \mathbf{r}_i} - \frac{\partial \hat{\Phi}^{(N)}}{\partial \mathbf{r}_i} \frac{\partial}{\partial \mathbf{p}_i} \right). \quad (14)$$

This equation is rewritten with use of Eqs. (11) and (12):

$$i\hat{L} = \hat{L}_0 + \hat{L}_m. \quad (15)$$

Here, time is scaled as

$$\hat{t} = t(\Lambda / m_0 d^2)^{1/2}, \quad (16)$$

and

$$i\hat{L}_0 = \sum_i \left( \hat{\mathbf{p}}_i \frac{\partial}{\partial \hat{\mathbf{r}}_i} - \frac{\partial \hat{\Phi}^{(N)}}{\partial \hat{\mathbf{r}}_i} \frac{\partial}{\partial \hat{\mathbf{p}}_i} \right),$$

$$i\hat{L}_m = - \sum_i \left( \hat{\mathbf{p}}_i \frac{\partial}{\partial \hat{\mathbf{r}}_i} \right) \mu_i. \quad (17)$$

The random force acting on the  $i$ th ion evolves according to the equation

$$\mathbf{f}_i(t) = \exp[i(1 - P)Lt] \mathbf{f}_i(0). \quad (18)$$

The reduced form of the above equation is

$$\hat{\mathbf{f}}_i(\hat{t}) = \exp[i(1 - \hat{P})\hat{L}\hat{t}] \hat{\mathbf{f}}_i(0), \quad (19)$$

where

$$\hat{\mathbf{f}}_i(\hat{t}) = \mathbf{f}_i(t) (d/\Lambda). \quad (20)$$

$P$  is the projection operator defined<sup>14</sup> by

$$P(\dots) = \mathbf{p}_i \langle \dots, \mathbf{p}_i \rangle / \langle \mathbf{p}_i, \mathbf{p}_i \rangle = \hat{\mathbf{p}}_i \langle \dots, \hat{\mathbf{p}}_i \rangle / \langle \hat{\mathbf{p}}_i, \hat{\mathbf{p}}_i \rangle = \hat{P}(\dots), \quad (21)$$

where the bra-ket represents the canonical average of the perturbed system.

The scaled Hamiltonian, evolution operator, and projection operator are affected by the scaled momentum, position, and time and also the perturbation parameter  $\mu_i$ . The canonical average of the perturbed system is rewritten as the sum of the canonical average of the unperturbed system and the polynomial with respect to  $\mu_i$ .<sup>7,8</sup> The  $\mu_i$  value satisfies

$$\mu_{i \in A} = \mu_A = \mu, \quad \mu_{i \in C} = \mu_C = -\mu, \quad \mu = \frac{m_A - m_C}{m_A + m_C}, \quad (22)$$

because the system to be considered is a binary mixture consisting of equal numbers of anion and cation.

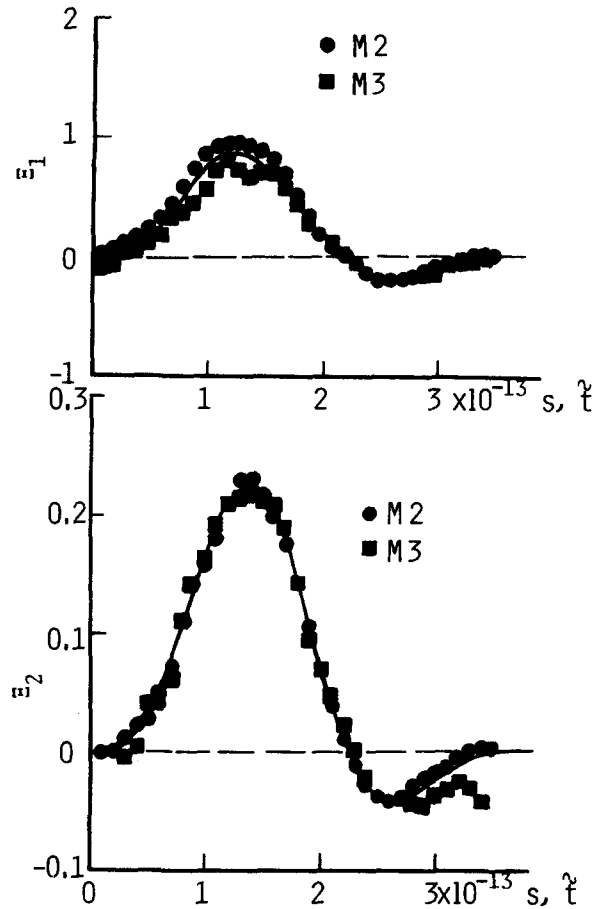


FIG. 7. Coefficients of the perturbation terms for the memory kernel.

Then, the normalized memory kernel can be described as

$$Y_\nu(\hat{t}) \equiv \frac{K_\nu(\hat{t})}{K_\nu(0)} = \frac{\langle \hat{\mathbf{f}}_i(\hat{t}) \hat{\mathbf{f}}_i(0) \rangle}{\langle \hat{\mathbf{f}}_i(0) \hat{\mathbf{f}}_i(0) \rangle} = Y_0(\hat{t}) + \sum_{n=1}^{\infty} c_n(\hat{t}) \mu_\nu^n, \quad i \in \nu,$$

$$Y_0(\hat{t}) = \frac{\langle \hat{\mathbf{f}}_{i0}(\hat{t}) \hat{\mathbf{f}}_{i0}(0) \rangle_0}{\langle \hat{\mathbf{f}}_{i0}(0) \hat{\mathbf{f}}_{i0}(0) \rangle_0}. \quad (23)$$

$\langle \rangle_0$  represents the canonical average of the unperturbed system. The  $c_n(\hat{t})$  terms are functions of the scaled time and are invariant for the ion species.

For the ECACF, the odd order terms with respect to  $\mu_\nu$  vanish because the electrical conduction process is not a singlet process but reflects the collective property, and Eq. (22) holds for univalent molten salts. Then,

$$Z^e(\hat{t}) = Z_0^e(\hat{t}) + s_2(\hat{t}) \mu^2 + s_4(\hat{t}) \mu^4 + O(\mu^6). \quad (24)$$

From Eq. (23) the following equations are obtained:

$$\Xi_1 = (Y_A + Y_C - 2Y_0) / 2\mu^2 = \sum_{n=1}^{\infty} c_{2n}(\hat{t}) \mu^{2n-2}, \quad (25a)$$

$$\Xi_2 = (Y_A - Y_C) / 2\mu = \sum_{n=1}^{\infty} c_{2n-1}(\hat{t}) \mu^{2n-2}. \quad (25b)$$

The  $\Xi_1$  and  $\Xi_2$  values for the runs M2 and M3 are shown in Fig. 7. The normalized memory kernel can be approximately described by using the first and sec-

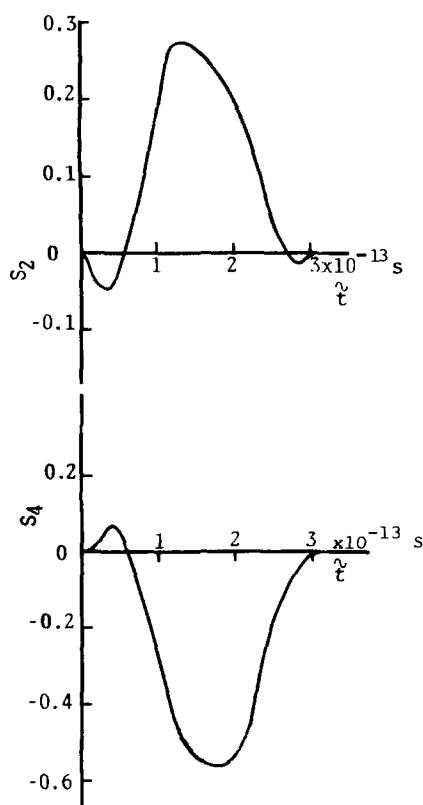


FIG. 8. Coefficients of the perturbation terms for ECACF.

ond orders of the perturbation. The coefficients  $c_1(\bar{t})$  and  $c_2(\bar{t})$  are determined as shown by the solid curves as an average.

The  $s_2$  and  $s_4$  values can be determined from the experimental results of the ECACF's if higher order terms  $O(\mu^6)$  in Eq. (24) are neglected. The resulting values of  $s_2$  and  $s_4$  are shown in Fig. 8.

The VACF's for the systems with unequal ionic masses can be evaluated from the normalized memory kernel for the unperturbed system with the help of the  $c_1$  and  $c_2$  values in Fig. 7 by using the numerical Fourier transform of Eq. (5a). The resulting VACF's are shown as the solid curves in Fig. 2 and these agree well with the experimental results except for the system of  $m_A/m_C = 10$ (M4). The ECACF's evaluated from Eq. (24) with the  $s_2$  and  $s_4$  values in Fig. 8 are also shown in Fig. 4 as the solid curves. The solid curves explain well the experimental results. This consistency ensures the validity of the present perturbation approach on the mass difference effect.

## V. SELF-DIFFUSION COEFFICIENT AND ELECTRICAL CONDUCTIVITY

The self-diffusion coefficient is described in terms of the friction coefficient:

$$D_\nu = \frac{kT}{m_\nu \zeta_\nu},$$

$$\zeta_\nu = \int_0^\infty K_\nu(t) dt$$

$$= K_\nu(0)(\Lambda/m_0 d^2)^{-1/2} \int_0^\infty Y_\nu(\hat{t}) d\hat{t}. \quad (26)$$

Equations (23) and (26) yield

$$\frac{kT}{D_\nu d} \left( \frac{\Lambda}{2m_\nu F_\nu^2} \right)^{1/2} = \frac{kT}{D_0 d} \left( \frac{\Lambda}{m_0 F_0^2} \right)^{1/2} + C_1 \mu_\nu + C_2 \mu^2, \quad (27)$$

where

$$C_1 = \int_0^\infty c_1(\hat{t}) d\hat{t}, \quad C_2 = \int_0^\infty c_2(\hat{t}) d\hat{t}. \quad (28)$$

The first term on the right-hand side of Eq. (27) represents the contribution of the unperturbed system and this is not an explicit function of the mass. Then,

$$1/\hat{D}_\nu \equiv \frac{kT}{D_\nu d} \left( \frac{\Lambda}{2m_\nu F_\nu^2} \right)^{1/2} = C_0 + C_1 \mu_\nu + C_2 \mu^2. \quad (29)$$

The coefficients  $C_i$ ,  $i=0-2$ , are functions of the state variables, the reduced temperature  $\hat{T}$ , and the reduced density  $\hat{\rho}$ :

$$\hat{T} = kTd/e^2, \quad \hat{\rho} = Nd^3/V. \quad (30)$$

This equation gives a simple law of corresponding states for molten salts, because the size effect of the ions is comparatively weak. The experimental results of the self-diffusion coefficient would be correlated with Eq. (27) or Eq. (29), which can be rewritten as

$$\frac{kT}{D_\nu} \left( \frac{m^*}{2m_\nu} \right)^{1/2} \frac{1}{F_\nu} = \frac{kT}{D_\nu^* F_\nu} + C_1' \mu_\nu + C_2' \mu^2, \quad (31)$$

where  $C_1'$  and  $C_2'$  are obtained by integrating  $c_1$  and  $c_2$  shown in Fig. 7:

$$C_1' = \int_0^\infty c_1(\bar{t}) d\bar{t} = 8.2 \times 10^{-15} \text{ s}, \quad (32)$$

$$C_2' = \int_0^\infty c_2(\bar{t}) d\bar{t} = 2.3 \times 10^{-14} \text{ s}, \quad \bar{t} = t(m^*/2m_\nu)^{1/2}.$$

Figure 9 shows the correlation of the experimental results according to Eq. (31). The solid line in the figure shows Eqs. (31) and (32) and fits well the experimental results.

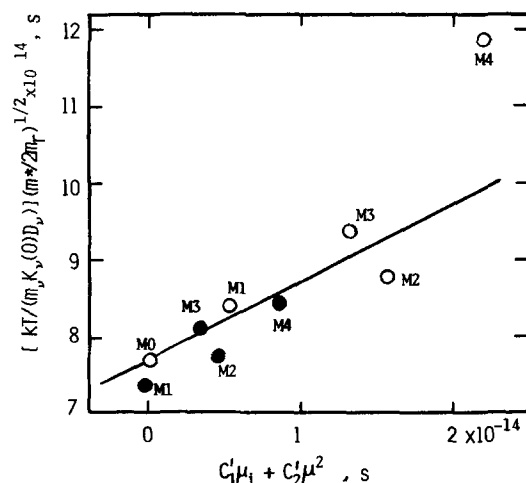


FIG. 9. Correlation of the self-diffusion coefficient. Solid line: Eq. (31); keys: experimental, open circle; anion, black circle; cation.

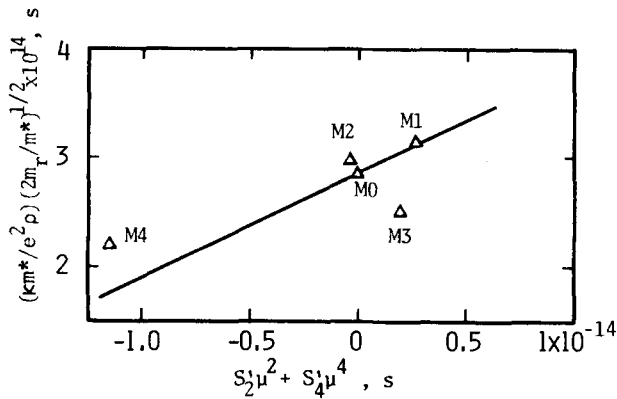


FIG. 10. Correlation of the electrical conductivity. Solid line: Eq. (35).

The electrical conductivity can be expressed by taking into account Eqs. (8) and (24):

$$\hat{\kappa} \equiv \frac{\kappa}{e^2 \rho d} (2\Lambda m_r)^{1/2} = S_0 + S_2' \mu^2 + S_4' \mu^4, \quad (33)$$

where

$$S_2' = \int_0^\infty s_2(\hat{t}) d\hat{t}, \quad (34)$$

$$S_4' = \int_0^\infty s_4(\hat{t}) d\hat{t}. \quad (34)$$

Equation (33) is rewritten in the form

$$\frac{\kappa m^*}{e^2 \rho} \left( \frac{2m_r}{m^*} \right)^{1/2} = \frac{\kappa^* m^*}{e^2 \rho} + S_2' \mu^2 + S_4' \mu^4. \quad (35)$$

The  $S_2'$  and  $S_4'$  values are determined from  $s_2$  and  $s_4$  in Fig. 8:

$$S_2' = \int_0^\infty s_2(\vec{t}) d\vec{t} = 3.2 \times 10^{-14} \text{ s},$$

$$S_4' = \int_0^\infty s_4(\vec{t}) d\vec{t} = -7.4 \times 10^{-14} \text{ s}. \quad (36)$$

Figure 10 shows the correlation of the electric conductivity with Eq. (35). The solid line in this figure shows Eqs. (35) and (36) and this agrees approximately with the experimental results. It can be concluded from the above agreements for the self-diffusion coefficient and the electrical conductivity that the present perturbation approach is valid for evaluating the transport properties of molten salts.

#### ACKNOWLEDGMENTS

The authors gratefully acknowledge the financial support from a grant in aid for scientific research from the Ministry of Education, Japan. The numerical calculations were performed at the Data Processing Center, Kyoto University.

- <sup>1</sup>M. P. Tosi and F. G. Fumi, *J. Phys. Chem. Solids* **21**, 45 (1964).
- <sup>2</sup>E. Helfand and S. A. Rice, *J. Chem. Phys.* **32**, 1642 (1962).
- <sup>3</sup>K. Tokubo, K. Nakanishi, and N. Watanabe, *J. Chem. Phys.* **67**, 4162 (1977).
- <sup>4</sup>R. E. Young and J. P. O'Connell, *Ind. Eng. Chem. Fundam.* **10**, 418 (1971).
- <sup>5</sup>G. Cicotti, G. Jacucci, and I. R. McDonald, *Phys. Rev. A* **13**, 426 (1976).
- <sup>6</sup>F. Lantelme, P. Turq, and P. Schofield, *Mol. Phys.* **31**, 1085 (1976).
- <sup>7</sup>I. Ebbsjo, P. Schofield, K. Skold, and I. Waller, *J. Phys. C* **7**, 3891 (1974).
- <sup>8</sup>M. Parrinello, M. P. Tosi, and N. H. March, *J. Phys. C* **7**, 2577 (1974).
- <sup>9</sup>L. Verlet, *Phys. Rev.* **159**, 98 (1967).
- <sup>10</sup>P. P. Ewald, *Ann. Phys. (Paris)* **21**, 1087 (1921).
- <sup>11</sup>Y. Nagamiya, *Kotairon II* (Kyoritsu, Tokyo, 1951).
- <sup>12</sup>A. Rahman, *Phys. Rev. Sect. A* **136**, 405 (1964).
- <sup>13</sup>R. Zwanzig, in *Lectures in Theoretical Physics*, edited by W. Brittin (Wiley-Interscience, New York, 1961), Vol. 3, pp. 106-141.
- <sup>14</sup>H. Mori, *Prog. Theor. Phys.* **33**, 423 (1965).
- <sup>15</sup>Y. Tada, M. Harada, and M. Tanigaki (unpublished).